Cavity-mediated cooling of a trapped Λ-type three-level atom using a standing-wave laser field

Zhen Yi and Gao-xiang Li*
Department of Physics, Huazhong Normal University, Wuhan 430079, China

Ya-ping Yang
Department of Physics, Tongji University, Shanghai 200092, China

(Received 5 February 2013; published 20 May 2013)

We propose a ground-state cavity-mediated cooling scheme for a trapped atom, which is in the Λ configuration and confined inside a high-finesse optical cavity, using a standing-wave cooling laser. The carrier transition can be prohibited by placing the atom at the node of the cavity field, and the blue-sideband transition can be simultaneously eliminated by exploiting quantum interference via tuning the frequency of the cooling laser. As a consequence, the ground-state cooling for the trapped atom can be achieved. Moreover, we numerically demonstrate the superiority by placing the atom at the antinode of the standing-wave cooling laser as compared with the running-wave cooling laser, and the robustness of the scheme using the standing-wave laser. Meanwhile, the cooling rate can reach the same order of magnitude as that obtained in the cavity–electromagnetically-induced-transparency cooling scheme, and the explicit expression for the final phonon number in higher order is also presented.

DOI: 10.1103/PhysRevA.87.053408 PACS number(s): 37.10.De, 37.10.Mn, 03.67.−a

I. INTRODUCTION

Laser cooling is now the basis of many areas of physics and technology, from the probe of quantum properties of matter [1], to atomic clocks with high accuracy [2], to the realization of an optical one-way barrier for neutral atoms [3]. Thus variants of cooling methods, such as Doppler cooling [4], Sisyphus cooling [5], dark-state cooling schemes [6,7], resolved-sideband cooling [8], etc., have been proposed to cool down the atoms or ions. These technical developments greatly promote atom manipulation and have opened a new period in cavity quantum electrodynamics (QED) experimentation, since a single emitter strongly coupled to optical resonators forms a promising basis for the implementation of quantum networks [9,10]. Therefore, the control of the motional degrees of an atom inside the resonator is a vital step in cavity-QED implementation in an optical domain. Cavity QED, as a workhorse of the investigation of open quantum systems, plays an important role in quantum information science and in the fundamental testing of quantum coherence and quantum measurement [11–13].

It has been experimentally demonstrated that quantum interference effects between the atomic states play a key role in the cooling of atoms or ions [14]. If the cavity field couples to the motion of the trapped atom, further quantum interference effects can emerge that will increase the cooling efficiency [15–18]. By combining the quantum interference [19] and the cavity QED, the phenomenon of cavity-induced electromagnetically induced transparency (EIT) has been exploited to obtain a ground-state cooling scheme with high cooling efficiency [20], which has been demonstrated in the experiment of confining a single cesium atom by a dipole trap inside a high-finesse optical resonator, in which theoretical predictions and experimental results show remarkable agreement [21]. These results open the possibility for the realization of an efficient photonic interface based on single atoms. However, due to the existence of the blue-sideband transition, the zero heating rate in the leading order of the Lamb-Dicke parameter cannot be achieved. For a ground-state cooling scheme for a trapped atom outside the optical resonator using EIT, in order to eliminate the blue-sideband transition, Zhang *et al*. proposed the cooling scheme using a standing-wave cooling laser [22]. In addition, in 1992, Cirac *et al*. [23] have pointed out that by locating the atom at the node or antinode of the standing-wave laser, substantial cooling behaviors can be explored, which are extremely different from that using the running-wave lasers. Thus employing a standing-wave laser can offer the opportunity to obtain the lower final temperature for a trapped atom or ion inside a high-finesse optical resonator.

In this paper, we present a ground-state cooling scheme for a trapped Λ-configuration atom confined inside a high-finesse optical cavity, which can be cooled down by using a standing-wave cooling laser. The carrier transition can be prohibited by placing the atom at the node of the cavity field, where the atom can not be irradiated by the field in the zeroth-order Lamb-Dicke parameters. In addition, the atom should be located at the antinode of the standing-wave cooling laser at the same time, where the atomic motion does not couple to the laser characterized by the leading order of the Lamb-Dicke parameters. Via tuning the frequency of the cooling laser so that the involved one cavity and two laser photons fulfill the three-photon resonance condition, the blue-sideband transition is eliminated by exploiting the quantum interference effect. Therefore, the ground-state cooling can be achieved in the leading-order expansion of the Lamb-Dicke parameter. More precisely, we present the explicit expression for the steady-state phonon number in the higher-order Lamb-Dicke parameter. The cooling rate can also reach the same order of magnitude as that obtained in the cavity-induced EIT scheme [20]. The paper is organized as follows: in Sec. II, the model is introduced and the master equation for the atomic motion is derived. In Sec. III, the cooling behavior is investigated in the perturbation method. The numerical simulations for the

*gaox@phy.ccnu.edu.cn

system are presented in Sec. IV and finally the conclusion is drawn in Sec. V.

II. THE MODEL

A. Basic equation

We consider a Λ-configuration atom confined inside a high-finesse optical cavity by an external harmonic trapping potential with frequency ν and irradiated by a standing-wave laser field of frequency ω_L, while the cavity is weakly pumped by another laser field with frequency ω_p and Rabi frequency Ω_p. The atomic center-of-mass oscillates in one dimension along the x axis and is initially centered at the node of the cavity field and the antinode of the standing-wave cooling laser at the same time. The physical setup and the atomic level configuration are sketched in Fig. 1. The atom is comprised of an upper state $|e\rangle$ with level frequency ω_e and two ground states $|g_1\rangle$ and $|g_2\rangle$ with level frequencies ω_1 and ω_2, respectively. The atomic dipole transition $|g_1\rangle \leftrightarrow |e\rangle$ is driven by the standing-wave laser field with Rabi frequency Ω_L, and the transition $|g_2\rangle \leftrightarrow |e\rangle$ is coupled to the field of the optical resonator of frequency ω_c with the strength $g(x)$. The decay of the optical cavity to the external environment is characterized by linewidth κ, and the excited state $|e\rangle$ dissipates into the state $|g_j\rangle$ with rate $\gamma_j (j = 1,2)$, where the total radiative linewidth

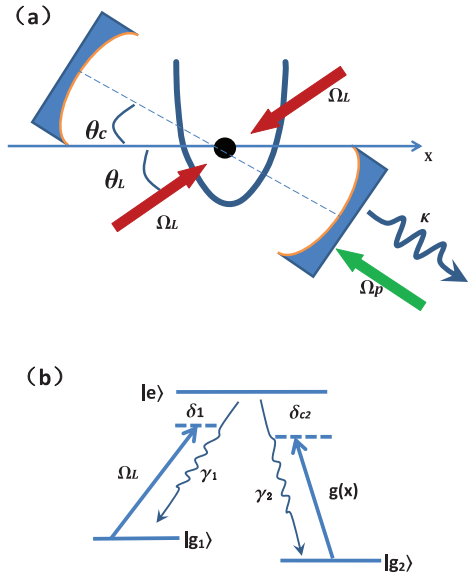

FIG. 1. (Color online) (a) The setup for the cooling dynamics of the center-of-mass motion of a trapped atom. The atom is confined inside a high-finesse optical cavity with coupling constant $g(x)$ and irradiated by a standing-wave laser field with Rabi frequency Ω_L. Initially, the atom is centered at the node of the cavity field and the antinode of the standing-wave cooling laser at the same time. The cavity is pumped by a weak laser field with strength Ω_p and decays with rate κ. $\theta_L(\theta_c)$ denotes the angle between the axis of the motion and the laser (cavity) wave vectors. (b) Relevant atomic transitions. Atomic transition $|g_1\rangle \to |e\rangle$ is driven by the standing-wave laser field, and the cavity field couples to the transition $|g_2\rangle \to |e\rangle$. δ_1 and δ_{c2} are the detunings between the photon fields and the corresponding atomic transitions. The excited state $|e\rangle$ dissipates spontaneously into states $|g_1\rangle$ and $|g_2\rangle$ with rates γ_1 and γ_2, respectively.

γ satisfies the relation $\gamma = \gamma_1 + \gamma_2$. In the frame of rotation with the lasers' frequencies, the Hamiltonian of this system is written as ($\hbar = 1$)

$$H = H_{\rm ext} + H_{\rm at} + H_{\rm cav} + H_{\rm L-cav} + H_{\rm L-at} + H_{\rm at-cav}, \quad (1)$$

where the individual Hamiltonians describing the external atomic motion, atomic internal degrees of freedom, and cavity mode in the right hand side are

$$\begin{aligned} H_{\rm ext} &= \nu\left(b^\dagger b + \tfrac{1}{2}\right), \\ H_{\rm at} &= -\delta_{c2}|e\rangle\langle e| + (\delta_1 - \delta_{c2})|g_1\rangle\langle g_1| + \Delta|g_2\rangle\langle g_2|, \\ H_{\rm cav} &= -\Delta a^\dagger a, \end{aligned} \quad (2)$$

and the laser-cavity, laser-atom, and cavity-atom interactions are described by

$$\begin{aligned} H_{\rm L-cav} &= \frac{\Omega_p}{2}(a + a^\dagger), \\ H_{\rm L-at} &= \frac{\Omega_L}{2}\cos(k_L \cos\theta_L x)(|e\rangle\langle g_1| + |g_1\rangle\langle e|), \\ H_{\rm at-cav} &= g(x)(|e\rangle\langle g_2|a + a^\dagger|g_2\rangle\langle e|). \end{aligned} \quad (3)$$

Here b and a are the annihilation operators of the phonon field describing the vibrational motion of the atom and cavity field, respectively. The detunings of cavity and laser fields from the corresponding atomic transitions are given by $\delta_{c2} = \omega_c - (\omega_e - \omega_2)$ and $\delta_1 = \omega_L - (\omega_e - \omega_1)$, respectively, while $\Delta = \omega_p - \omega_c$ is the detuning of pumping laser from the cavity field. The coupling coefficient between the cavity field and the atom is $g(x) = g\sin(k_c \cos\theta_c x)$, where $k_c(k_L)$ is the wave number of the cavity mode (the laser field), and $\theta_c(\theta_L)$ gives the orientation of the cavity wave vector (laser field vector) with respect to the axis of motion. The atom's position operator x is expressed as $x = \xi(b + b^\dagger)$, where $\xi = \sqrt{\hbar/2M\nu}$ denotes the size of the ground-state wave packet with M the mass of the atom.

The time-dependent system is described by the master equation

$$\frac{d}{dt}\rho = -i[H,\rho] + \mathcal{L}\rho + \mathcal{K}\rho, \quad (4)$$

where the atomic dissipations and the cavity decay are described by the Liouvillian operators

$$\begin{aligned} \mathcal{L}\rho &= \sum\nolimits_j \frac{\gamma_j}{2}(2|g_j\rangle\langle e|\tilde{\rho}|e\rangle\langle g_j| - |e\rangle\langle e|\rho - \rho|e\rangle\langle e|), \\ \mathcal{K}\rho &= \frac{\kappa}{2}(2a\rho a^\dagger - a^\dagger a\rho - \rho a^\dagger a), \end{aligned} \quad (5)$$

with γ_j and κ the damping rates of the excited atomic level and photons, respectively, and $\tilde{\rho}$ indicating the atomic motional recoil due to the emission of a photon, related to the angular distribution $\mathcal{N}_j(\theta)$ by the expression [24]

$$\tilde{\rho} = \int_{-1}^{1} \mathcal{N}_j(\theta) e^{ik_j x\cos\theta} \rho e^{-ik_j x\cos\theta} d\cos\theta. \quad (6)$$

Note that $\mathcal{N}_j(\theta)$ are evaluated by taking into account the geometry of the setup.

In the following, we assume that the strength of the laser driving the cavity is sufficiently weak and in the regime that the average photon number of the cavity mode $|\epsilon|^2 \equiv |\frac{\Omega_p/2}{\Delta + i\kappa/2}|^2$ is much smaller than unity. Therefore, it is feasible to investigate

the cooling dynamics in the cavity-atom Hilbert space that contains at most one excitation of the cavity mode, which is spanned by a group of states

$$\{|e,0\rangle,|g_1,0\rangle,|g_2,0\rangle,|g_2,1\rangle\}. \tag{7}$$

For later convenience we denote the states in the form: $|e,0\rangle \equiv |e\rangle$, $|g_1,0\rangle \equiv |g_1\rangle$, $|g_2,0\rangle \equiv |g_2\rangle$, and $|g_2,1\rangle \equiv |1\rangle$. Within these states, we rewrite $H_{\mathrm{L-cav}}$ and $H_{\mathrm{at-cav}}$ in Eq. (3) and the superoperators $\mathcal{K}\rho$ in Eq. (5) as

$$\begin{aligned} H_{\text{L-cav}} &= \frac{\Omega_p}{2}(|g_2\rangle\langle 1| + |1\rangle\langle g_2|), \\ H_{\text{at-cav}} &= g(x)(|e\rangle\langle 1| + |1\rangle\langle e|), \\ \mathcal{K}\rho &= \frac{\kappa}{2}(2|g_2\rangle\langle 1|\rho|1\rangle\langle g_2| - |1\rangle\langle 1|\rho - \rho|1\rangle\langle 1|), \end{aligned} \tag{8}$$

and the sum of the Hamiltonians H_{at} and H_{cav} becomes the same form as H_{at} because of the zero energy frequency of the state $|g_2,1\rangle$ in the rotating frame, while the other terms remain unchanged.

B. Reduced master equation for atomic motion in the Lamb-Dicke limit

In the Lamb-Dicke regime, we expand the Hamiltonian up to the first order of the Lamb-Dicke parameter $\eta = k\sqrt{\hbar/2Mv}$, which scales the mechanical effects of light on the atomic motion. We define $\eta_L = \eta\cos\theta_L$ and $\eta_c = \eta\cos\theta_c$ to characterize the mechanical effects induced by the cooling laser and cavity field, respectively, where we have assumed that wave numbers of cavity k_c and the laser k_L are approximately equal: $k \approx k_c \approx k_L$. Thus the Hamiltonian comes into the form

$$H = H_{\mathrm{ext}} + H_0 + H_1, \tag{9}$$

where H_0 is the Hamiltonian in the zeroth-order expansion of η and is given by

$$\begin{aligned} H_0 = &-\delta_{c2}|e\rangle\langle e| + (\delta_1 - \delta_{c2})|g_1\rangle\langle g_1| + \Delta|g_2\rangle\langle g_2| \\ &+ \frac{\Omega_p}{2}(|g_2\rangle\langle 1| + |1\rangle\langle g_2|) + \frac{\Omega_L}{2}(|e\rangle\langle g_1| + |g_1\rangle\langle e|), \end{aligned} \tag{10}$$

while H_1 is the Hamiltonian in the first-order expansion of η and is written in the form $H_1 = V_1(b + b^\dagger)$, in which

$$V_1 = \eta_c g(|e\rangle\langle 1| + |1\rangle\langle e|). \tag{11}$$

Then we can rewrite the master equation of this system as

$$\frac{d}{dt}\rho = \mathcal{L}_{0e}\rho + \mathcal{L}_0\rho + \mathcal{L}_1\rho + \mathcal{L}_2\rho, \tag{12}$$

where the zeroth-order Liouvillian operators

$$\mathcal{L}_0\rho = -i[H_0,\rho] + \mathcal{L}_{0s}\rho + \mathcal{K}\rho \tag{13}$$

describe the internal atomic and cavity degrees of freedom without coupling to the phonon mode and

$$\mathcal{L}_{0s}\rho = \sum\nolimits_j \frac{\gamma_j}{2}(2|g_j\rangle\langle e|\rho|e\rangle\langle g_j| - |e\rangle\langle e|\rho - \rho|e\rangle\langle e|) \tag{14}$$

represents the atomic spontaneous emission without the influence of the recoils by the emission of photons. The Liouvillian operators

$$\mathcal{L}_{0e}\rho = -i[H_{\mathrm{ext}},\rho] \tag{15}$$

and

$$\mathcal{L}_1\rho = -i[H_1,\rho] \tag{16}$$

describe the vibrational motion of the trapped atom and the mechanical effect on the atom induced by the cavity field. The remaining Liouvillian operator

$$\begin{aligned} \mathcal{L}_2\rho = &\sum\nolimits_j \alpha_j \frac{\gamma_j}{2}\eta_j^2|g_j\rangle\langle e|(b\rho b^\dagger + b^\dagger\rho b \\ &- bb^\dagger\rho - b^\dagger b\rho + \text{H.c.})|e\rangle\langle g_j| \end{aligned} \tag{17}$$

describes the diffusion caused by the recoils of the emission of photons, with

$$\alpha_j = \int_{-1}^{1} d\cos\theta\cos^2\theta\mathcal{N}_j(\theta) \tag{18}$$

the angular dispersion of the atom momentum due to the spontaneous emission of photons and equal to $\frac{2}{5}$ for the usual dipole transition [24]. By adiabatically eliminating the internal atomic and cavity degrees of freedom and making use of the second-order perturbation method with respect to η [23], we obtain the time-dependent reduced density matrix for the phonon mode μ in the form

$$\begin{aligned} \frac{d}{dt}\mu = &[S(\nu) + D](b\mu b^\dagger - b^\dagger b\mu) + [S(-\nu) + D] \\ &\times (b^\dagger\mu b - bb^\dagger\mu) + \text{H.c.}, \end{aligned} \tag{19}$$

where $S(\nu)$ is the two-time correlation function of atomic and cavity operators and D is the diffusion coefficient, which are, respectively, expressed as

$$\begin{aligned} S(\nu) &= \int_0^\infty dt e^{i\nu t}\langle V_1(t)V_1(0)\rangle_{\mathrm{st}}, \\ D &= \sum\nolimits_j \alpha_j \frac{\gamma_j}{2}\eta_j^2 \mathrm{Tr}\{\sigma_{eg_j}\sigma_{g_je}\rho_{\mathrm{st}}\}. \end{aligned} \tag{20}$$

It is noted that the transition operators are $\sigma_{mn} = |m\rangle\langle n|$, where $\{|m\rangle,|n\rangle\} = \{|e\rangle,|g_1\rangle,|g_2\rangle,|1\rangle\}$.

C. Rate equation

According to Eq. (19), one can directly derive the rate equation for the occupation probability $p_n = \langle n|\mu|n\rangle$ of the phonon number state $|n\rangle$ as

$$\begin{aligned} \frac{d}{dt}p_n = &(n+1)A_-p_{n+1} - [(n+1)A_+ + nA_-]p_n \\ &+ nA_+p_{n-1}, \end{aligned} \tag{21}$$

where

$$A_\pm = 2\mathrm{Re}\{S(\mp\nu) + D\} \tag{22}$$

are the heating and cooling coefficients. Hence the mean phonon number $\langle n\rangle$ with the time evolution obeys the equation

$$\langle\dot{n}\rangle = -(A_- - A_+)\langle n\rangle + A_+. \tag{23}$$

Then we can easily obtain the steady-state mean phonon number and cooling rate

$$n_{\mathrm{st}} = \frac{A_+}{A_- - A_+}, \quad W = A_- - A_+, \tag{24}$$

respectively. Obviously, when the heating coefficient A_+ becomes zero, the mean phonon number arrives at zero in the long time limit.

III. ANALYSIS OF CAVITY-MEDIATED COOLING BEHAVIOR FOR THE TRAPPED ATOM IN THE PERTURBATION METHOD

A. Explicit expressions for the heating and cooling coefficients

By using the quantum regression theory [25], the two-time correlation function $S(\nu)$ can be calculated from single-time averages $\langle\sigma_{mn}\rangle = \mathrm{Tr}\{|m\rangle\langle n|\rho\}$, and the time evolution of these elements can be derived from Eq. (13) and governed by the equations

$$\begin{aligned}
\langle\dot{\sigma}_{ee}\rangle &= -\gamma\langle\sigma_{ee}\rangle + i\frac{\Omega_L}{2}(\langle\sigma_{g_1e}\rangle - \langle\sigma_{eg_1}\rangle),\\
\langle\dot{\sigma}_{g_1g_1}\rangle &= \gamma_1\langle\sigma_{ee}\rangle + i\frac{\Omega_L}{2}(\langle\sigma_{eg_1}\rangle - \langle\sigma_{g_1e}\rangle),\\
\langle\dot{\sigma}_{g_1e}\rangle &= \left(i\delta_1 - \frac{\gamma}{2}\right)\langle\sigma_{g_1e}\rangle + i\frac{\Omega_L}{2}(\langle\sigma_{ee}\rangle - \langle\sigma_{g_1g_1}\rangle),\\
\langle\dot{\sigma}_{11}\rangle &= -\kappa\langle\sigma_{11}\rangle + i\frac{\Omega_p}{2}(\langle\sigma_{g_21}\rangle - \langle\sigma_{1g_2}\rangle),\\
\langle\dot{\sigma}_{g_2g_2}\rangle &= \kappa\langle\sigma_{11}\rangle + \gamma_2\langle\sigma_{ee}\rangle + i\frac{\Omega_p}{2}(\langle\sigma_{1g_2}\rangle - \langle\sigma_{g_21}\rangle),\\
\langle\dot{\sigma}_{g_21}\rangle &= \left(i\Delta - \frac{\kappa}{2}\right)\langle\sigma_{g_21}\rangle + i\frac{\Omega_p}{2}(\langle\sigma_{11}\rangle - \langle\sigma_{g_2g_2}\rangle),\\
\langle\dot{\sigma}_{1e}\rangle &= \left(i\delta_{c2} - \frac{\gamma+\kappa}{2}\right)\langle\sigma_{1e}\rangle - i\frac{\Omega_L}{2}\langle\sigma_{1g_1}\rangle + i\frac{\Omega_p}{2}\langle\sigma_{g_2e}\rangle,\\
\langle\dot{\sigma}_{1g_1}\rangle &= \left[i(\delta_{c2}-\delta_1) - \frac{\kappa}{2}\right]\langle\sigma_{1g_1}\rangle - i\frac{\Omega_L}{2}\langle\sigma_{1e}\rangle + i\frac{\Omega_p}{2}\langle\sigma_{g_2g_1}\rangle,\\
\langle\dot{\sigma}_{g_2e}\rangle &= \left[i(\delta_{c2}+\Delta) - \frac{\gamma}{2}\right]\langle\sigma_{g_2e}\rangle - i\frac{\Omega_L}{2}\langle\sigma_{g_2g_1}\rangle + i\frac{\Omega_p}{2}\langle\sigma_{1e}\rangle,\\
\langle\dot{\sigma}_{g_2g_1}\rangle &= i(\Delta-\delta_1+\delta_{c2})\langle\sigma_{g_2g_1}\rangle - i\frac{\Omega_L}{2}\langle\sigma_{g_2e}\rangle + i\frac{\Omega_p}{2}\langle\sigma_{1g_1}\rangle.
\end{aligned} \tag{25}$$

However, because of the small laser-cavity coupling strength, it is adequate to employ the perturbation method in Ω_p, and then we can obtain the analytical expressions of heating and cooling coefficients $A_\pm$ in Eq. (22) in the order $\Omega_p^2\eta^2$ by neglecting the terms in higher orders. In the following we use $\langle\sigma_{mn}^{(i)}\rangle (i = 0,1,2)$ to indicate the ith order of the averages in Ω_p. For steady-state solutions in the zeroth order of Ω_p, we can easily obtain $\langle\sigma_{g_2g_2}^{(0)}(\infty)\rangle = 1$ and the other elements are equal to zero, which coincides with the physical situation that when there is no laser driving on the cavity mode, the cavity field is in a vacuum and the atom stays in its ground state at the steady state of the system.

Then the first-order steady-state solutions $\langle\sigma_{mn}^{(1)}(\infty)\rangle$ can be obtained by substituting $\langle\sigma_{g_2g_2}^{(0)}(\infty)\rangle = 1$ into Eq. (25), which are given by

$$\langle\sigma_{g_21}^{(1)}(\infty)\rangle = \frac{i\Omega_p/2}{i\Delta - \kappa/2}, \quad \langle\sigma_{1g_2}^{(1)}(\infty)\rangle = \frac{i\Omega_p/2}{i\Delta + \kappa/2}, \tag{26}$$

and all the other first-order terms are zero. Following the same procedure, we can obtain the second-order steady-state solution

$$\langle\sigma_{11}^{(2)}(\infty)\rangle = \frac{\Omega_p^2/4}{\Delta^2 + \kappa^2/4} \tag{27}$$

with all the other solutions zero. Since the atom is located at the node of the cavity field, the cavity field can not drive transition $|1\rangle \to |e\rangle$. Thus the population in the state $|e\rangle$ is zero and the diffusion term D that is proportional to the steady-state population in state $|e\rangle$ also becomes zero.

By making use of the quantum regression theorem, the two-time correlation function $S(\pm\nu)$ can be obtained after some calculations. And then $A_\pm$ can be immediately calculated and written in the form

$$A_\pm = \frac{g^2\eta_c^2|\epsilon|^2\gamma(\Delta - \delta_1 + \delta_{c2} \mp \nu)^2}{f(\Delta \mp \nu)}, \tag{28}$$

where the denominator is

$$\begin{aligned}
f(\Delta \mp \nu) = &\left[(\Delta + \delta_{c2} \mp \nu)(\Delta - \delta_1 + \delta_{c2} \mp \nu) - \frac{\Omega_L^2}{4}\right]^2\\
&+ \frac{\gamma^2}{4}(\Delta - \delta_1 + \delta_{c2} \mp \nu)^2.
\end{aligned} \tag{29}$$

It is obvious that the heating coefficient A_+ becomes zero when the relation $\delta_1 = \Delta + \delta_{c2} - \nu$ in the leading order of the expansion in η, which means that both the carrier- and blue-sideband transitions are eliminated. Meanwhile the cooling rate $W = A_- - A_+$ is given by

$$W = \frac{4g^2\eta_c^2|\epsilon|^2\gamma\nu^2}{\left[2\nu(2\nu + \delta_1) - \frac{\Omega_L^2}{4}\right]^2 + \gamma^2\nu^2}. \tag{30}$$

We can easily find out that the maximal value of W is taken under the condition $2\nu(2\nu + \delta_1) = \frac{\Omega_L^2}{4}$. Therefore, the detunings of the laser and cavity fields from the atomic transitions should satisfy the equations

$$\delta_1 = -2\nu + \frac{\Omega_L^2}{8\nu}, \quad \delta_{c2} = -\Delta - \nu + \frac{\Omega_L^2}{8\nu}, \tag{31}$$

and the cooling rate becomes

$$W = \frac{4g^2\eta_c^2|\epsilon|^2}{\gamma}, \tag{32}$$

with

$$|\epsilon|^2 = \left|\frac{\Omega_p/2}{\Delta + i\kappa/2}\right|^2 \tag{33}$$

the mean number of intracavity photons when no atom is present.

B. Cooling and heating scattering processes

In order to acquire the physical insight into the cooling scheme, especially the success in eliminating heating processes in theory, we sketch the heating and cooling scattering processes in Fig. 2, where $|n\rangle$ represents the phonon number state. In the following we will illustrate the scattering processes to explain how the scheme can succeed in the elimination of carrier- and blue-sideband transitions. Initially, the system is in the state $|g_2\rangle$ and transits into the state $|1\rangle$ via irradiation of the

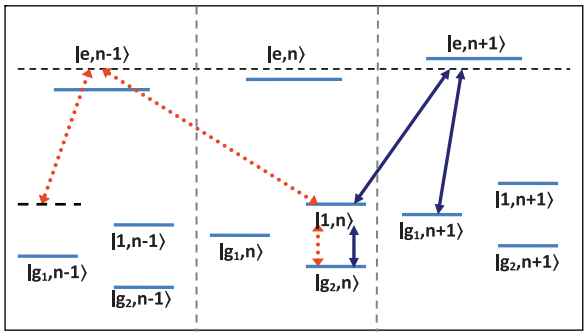

FIG. 2. (Color online) Schematic illustration of the cooling and heating scattering processes. The carrier transition $|g_2\rangle \to |1\rangle \to |e\rangle$ is prohibited by locating the atom at the node of the cavity field. The blue-sideband transition $|g_2,n\rangle \to |1,n\rangle \to |e,n+1\rangle$ can destructively interfere with the transition $|g_1,n+1\rangle \to |e,n+1\rangle$ leading to the elimination of the transition, which is shown by the blue solid lines. The cooling transition is shown by the red dotted lines.

driving laser with strength Ω_p. Due to the location of the atom at the node of the cavity field, the carrier transition $|1\rangle \to |e\rangle$ is prohibited. In addition, the blue-sideband transition $|g_2,n\rangle \to |1,n\rangle \to |e,n+1\rangle$ mediated by the cavity field can destructively interfere with the transition $|g_1,n+1\rangle \to |e,n+1\rangle$ that is driven by the standing-wave laser with strength Ω_L, under the condition that the involved one cavity photon and two laser photons fulfill the three-photon resonance, i.e., $\delta_1 = \Delta + \delta_{c2} - \nu$. The complete destructive interference leads to the elimination of the blue-sideband transition, which is indicated by the blue solid lines in Fig. 2. Via utilizing the quantum interference in the blue-sideband transition, none of the population injects into the states $|e,n+1\rangle$ and $|1,n+1\rangle$. Therefore, the heating scattering cannot occur and the coefficient A_+ can achieve zero.

As compared with the ongoing EIT-control of a single atom in an optical resonator, in which the results can set the basis to the realization of the photonic interface based on the cooled single atoms, we obtain a zero heating rate in the leading order of Lamb-Dicke parameters, which can be considered as an improvement on the experiment. Meanwhile, the cooling scattering process is indicated by the red dotted lines. Because of the prohibition of the transition $|e,n-1\rangle \leftrightarrow |1,n-1\rangle$ by locating the atom at the node of the cavity field, there is no population injection into the state $|1,n-1\rangle$, leading to no cooling scattering via the cavity decay κ, which coincides with the cooling rate in Eq. (28). However, in the limit $\gamma \gg \kappa$, the cooling rate can still reach the same order of magnitude as that obtained in the cavity-induced EIT scheme in the case of a far-off resonant [20].

Distinct from the results in Ref. [22], where via utilizing two-photon resonance heating scattering is prohibited, in this paper one cavity photon is involved to form three-photon resonance to eliminate the blue-sideband transition. The obtained cooling limits of atomic motion are both zero in the zeroth order of the Lamb-Dicke parameter, and cooling rates are in the same form by letting $\epsilon g = \Omega_g$ therein. However, in a higher order of the Lamb-Dicke parameter, we will show that the cooling behavior is related to the cavity.

IV. NUMERICAL SIMULATIONS

In order to compare the cooling behavior with standing-wave laser, we apply a running-wave cooling laser to couple the atomic transition $|g_1\rangle \leftrightarrow |e\rangle$. The Hamiltonian in zeroth order of η is unchanged while the mechanical effects on the atomic motion are governed by a new Hamiltonian $H_1' = V_1'(b + b^\dagger)$ with

$$V_1' = \eta_c g(|e\rangle\langle 1| + |1\rangle\langle e|) + i\eta_L \frac{\Omega_L}{2}(|e\rangle\langle g_1| - |g_1\rangle\langle e|), \quad (34)$$

where η_L characterizes the mechanical effect caused by the running-wave laser. Following the same procedure as above, it can be verified that the new heating and cooling coefficients $A_\pm$ are the same form as Eq. (28) up to the order of $\Omega_p^2\eta^2$ and thus the zero cooling limit can be also achieved in the order of $O(\Omega_p^2\eta^2)$. However, the differences in higher order on the cooling behavior between standing- and running-wave lasers will be numerically shown in the following.

We follow the parameters taken in the EIT-control experiment of a cesium atom [21], in which the atom is located in a dipole trap and subsequently transported into a high-finesse cavity. The trap frequency and damping rate are, respectively, $\nu/2\pi = 0.2$ MHz and $\kappa/2\pi = 0.4$ MHz. The relevant Λ-configuration atomic levels are comprised of the hyperfine ground states $|g_{1,2}\rangle = |^2S_{1/2}, F = 3,4\rangle$ and the excited state $|e\rangle = |^2P_{3/2}, F = 4\rangle$. With the fixed experimental parameters $\gamma/2\pi = 2.6$ MHz, $\Omega_p/2\pi = 0.23$ MHz, $\Omega_L/2\pi = 2.8$ MHz, $\Delta/2\pi = 2.3$ MHz, and $g/2\pi = 3.6$ MHz. The mean intracavity photon number 2.5×10^{-3} validates the assumption that there is at most one photonic excitation in the cavity-atom system, and the values of two detunings δ_1, δ_{c2} are determined by Eq. (31). The Lamb-Dicke parameters are $\eta_c = \eta_L = 0.1$ along the cavity and laser wave vectors [24]. With these parameters, we carry out a numerical simulation by directly calculating the master equation in Eq. (12) in a truncated basis with $N = 10$ phononic excitations [26], which is presented in Fig. 3. Dashed curve (i) displays the cooling by using a running wave to couple the transition $|g_1\rangle \leftrightarrow |e\rangle$, where the final phonon number achieves about 1.37×10^{-3}. Solid curve (ii) displays the cooling by using a standing wave to drive the transition $|g_1\rangle \leftrightarrow |e\rangle$, and the final phonon number achieves a lower value of about 8.7×10^{-4}. The dash-dotted line (iii) is plotted with the analytical time-dependent solution of the phonon number determined by Eq. (23), which shows a match with the numerical simulation in curve (ii). Comparing curve (i) with (ii), we can easily find that for the standing-wave laser case the final phonon number is lower and the cooling rate is faster than those for the running-wave laser case. Although the cooling limits are both zero in the order $O(\Omega_p^2\eta_c^2)$, the differences can be numerically shown which are caused by the higher-order scattering processes.

In order to clearly see the higher-order scattering processes on the cooling behavior, especially the exact numerical result in final phonon population different from zero, which is obtained analytically in the order of $O(\Omega_p^2\eta^2)$, we calculate the cooling limit for the atomic motion to a higher order in $\Omega_p^2\eta^2$ for the standing-wave case. For the much low phonon occupation shown numerically, it is adequate to calculate the steady state of the system within the space containing at most one phonon

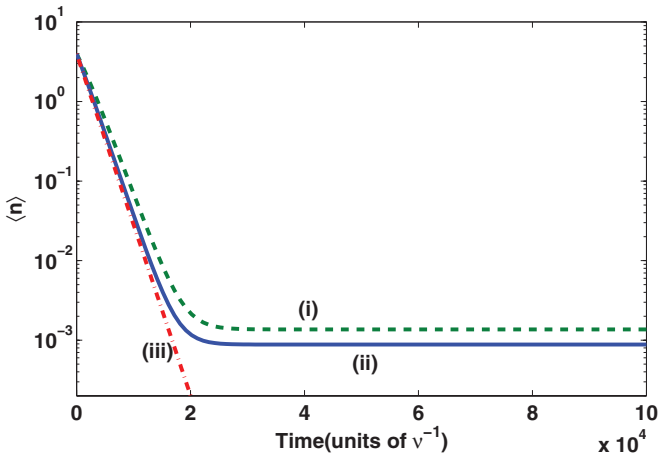

FIG. 3. (Color online) Numerical simulation of the cooling dynamics with the parameters: $\nu/2\pi = 0.2$ MHz, $\kappa/2\pi = 0.4$ MHz, $\gamma/2\pi = 2.6$ MHz, $\Omega_p/2\pi = 0.23$ MHz, $\Omega_L/2\pi = 2.8$ MHz, $\Delta/2\pi = 2.3$ MHz, and $g/2\pi = 3.6$ MHz, and $\eta_c = \eta_L = 0.1$. The values of two detunings are determined by Eq. (31). In dashed curve (i), the running-wave cooling laser is applied, and in solid curve (ii), the standing-wave cooling laser is applied. The dash-dotted line (iii) shows the analytical result governed by Eq. (23).

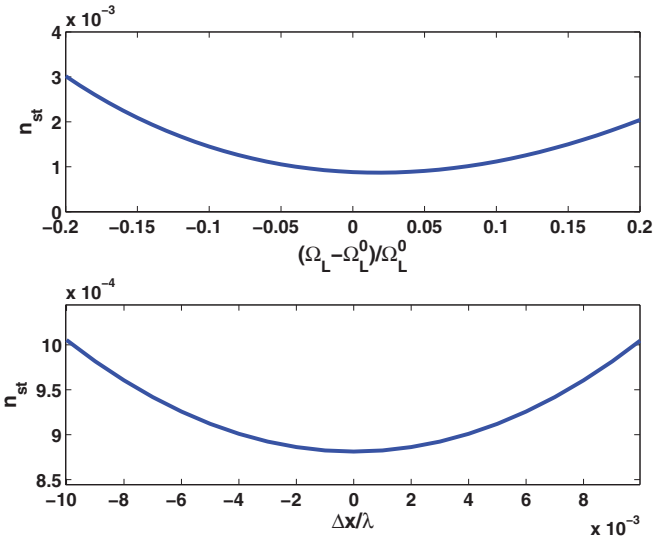

FIG. 4. (Color online) Numerical simulations of the final phonon number $n_{\rm st}$ as a function of Ω_L with the atom fixed at the node of the cavity field and the antinode of the laser field in (a) and the phase deviation of the atom with the cooling laser strength $\Omega_L/2\pi = 2.8$ MHz in (b). The parameters are $\nu/2\pi = 0.2$ MHz, $\kappa/2\pi = 0.4$ MHz, $\gamma/2\pi = 2.6$ MHz, $\Omega_p/2\pi = 0.23$ MHz, $\Omega_L^0/2\pi = 2.8$ MHz, $\Delta/2\pi = 2.3$ MHz, and $g/2\pi = 3.6$ MHz, and $\eta_c = \eta_L = 0.1$.

excitation. The space is spanned by the states $|i,j\rangle$, in which $|i\rangle$ is the cavity-atom states shown by Eq. (7) and $|j\rangle(j = 0,1)$ is the phonon number states. The time evolution for the elements of the density matrix $\rho_{ij,i'j'}$ is governed by the master equation in Eq. (12), which contains 64 equations. Under the assumptions of three-photon resonance $\delta_1 = \Delta + \delta_{c2} - \nu$ and the mean number of intracavity photons $|\epsilon|^2$ much lower, the steady state of the system is approximated in the form

$$\rho_{\rm st} \approx |\Psi\rangle\langle\Psi| + P^{(11)}_{g_2g_2}|g_2,1\rangle\langle g_2,1| + O\left(\Omega_p^4\eta_c^2\right) + O\left(\Omega_p^2\eta_c^4\right) \tag{35}$$

with the state function

$$|\Psi\rangle = |g_2,0\rangle + \frac{\Omega_p/2}{h(\Delta)}|1,0\rangle - \frac{g\eta_c\Omega_p}{\Omega_L h(\Delta)}|g_1,1\rangle + O\left(\eta_c^2\right), \tag{36}$$

and the population probability on state $|g_2,1\rangle$

$$P^{(11)}_{g_2g_2} = \frac{4\kappa|\epsilon|^2}{\gamma\Omega_L^2}\left\{\frac{\frac{\gamma^2}{4}+\nu^2}{|h(\Delta)|^2}|h(\Delta-\nu)|^2 + \frac{2\nu g^2\eta_c^2}{|h(\Delta)|^2} \times\left[\Delta-\nu+\frac{\kappa}{2\nu\gamma}\left(\frac{\gamma^2}{4}-\nu^2\right) + \frac{\kappa}{\gamma}(2\Delta-\nu)\frac{\nu^2+\frac{\gamma^2}{4}}{|h(\Delta)|^2}\right]\right\}. \tag{37}$$

Here $h(\Delta) = \Delta + i\kappa/2$ and we omit the normalization, and the cooling limit for the atomic motion is about

$$n_{\rm st} \approx \frac{(g\eta_c\Omega_p)^2}{\Omega_L^2|h(\Delta)|^2} + P^{(11)}_{g_2g_2}. \tag{38}$$

Therefore, in the higher order of $\Omega_p^2\eta^2$, the cooling behavior is related to the cavity. For example, the large cavity dissipation rate κ may prevent a lower cooling limit and the high-Q cavity will benefit for a lower cooling result. Distinct from the results in Ref. [22], the cooling limit in Eq. (38) can explicitly show the role that the cavity plays in the cooling behavior in the higher-order scattering processes.

It can be verified that our cooling scheme using the standing-wave laser is also robust against the fluctuation of Rabi frequencies and the position deviation of the atom. In Fig. 4(a) we numerically simulate the final phonon number with the change of the Rabi frequency Ω_L of the standing-wave laser that couples the transition $|e\rangle \leftrightarrow |g_1\rangle$. It can be seen that when the fluctuations of the Rabi frequencies are about 10%, the final phonon number may be affected in the range of about 10^{-3}. For the more realistic Rabi frequency fluctuations of about 2%, the final phonon number will keep in a higher order of precision. In addition, in our scheme it is required that the atom should be located at the node of the cavity field and the antinode of the cooling laser. However, the atom can not be fixed even if the position of the atom within the standing wave can be determined with a precision of up to $\lambda/100$ in the experimental realization [27]. In Fig. 4(b) the numerical simulation of the final phonon number as a function of the position deviation of the atom is presented. When the position error reaches up to 1% of the wavelength, the final phonon number is only affected in the range of the order of magnitude 10^{-4}. Note that when the atom is deviated from the fixed position, the cavity field dissipation channel will be involved in the scattering processes. This numerical result will also indicate the cavity-QED effect on the laser cooling.

Finally, it should be pointed out that even though the cooling limits induced by the standing- and running-wave cooling lasers are not distinguished from each other in the order of $O(\Omega_p^2\eta^2)$, they are different in higher-order processes. For example, for the transition into the state $|g_1,n+1\rangle$ in the order of $\Omega_p^2\eta^2$, in the running-wave case higher-order heating

transition into the excited state will be induced while in the standing-wave case by locating the atom at the antinode the heating transition can be suppressed because of the different mechanical effects on the atom described in Eqs. (34) and (11). This also coincides with the numerical results, which can demonstrate the superiority of the scheme by locating the atom at the antinode of the standing-wave cooling laser.

V. CONCLUSION

In summary, we have proposed a ground-state cooling scheme for a trapped Λ-configuration atom confined inside a high-finesse cavity by using a standing-wave cooling laser. Two heating mechanisms, the carrier- and the blue-sideband transitions, can be simultaneously eliminated. The carrier transition can be prohibited by placing the atom at the node of the cavity field, where the atom can not be irradiated by the cavity field in the zeroth-order Lamb-Dicke parameter. In addition, the atom has been simultaneously located at the antinode of the standing-wave cooling laser, where the laser cannot couple to the atomic motion in the leading order of Lamb-Dicke parameters. Via tuning the frequency of the cooling laser to make the involved one cavity and two laser photons satisfy the three-photon resonance condition, the blue-sideband transition is eliminated by exploiting the quantum destructive interference. Therefore, the motional ground state can be achieved in the leading-order expansion of the Lamb-Dicke parameter. We also present the more precise cooling limit in the higher order. Moreover, the cooling rate can reach the same order of magnitude as that obtained in the cavity-induced EIT cooling scheme in the case of a far-off resonant.

ACKNOWLEDGMENTS

This work is supported by the National Basic Research Program of China (Grant No. 2012CB921602), the National Natural Science Foundation of China (Grants No. 11074087 and No. 61275123), the Nature Science Foundation of Wuhan City (Grant No. 201150530149), and the Key Laboratory of Advanced Micro-Structure Materials of Tongji University.

[1] S. Chu, Rev. Mod. Phys. **70**, 685 (1998).
[2] W. H. Oskay, S. A. Diddams, E. A. Donley, T. M. Fortier, T. P. Heavner, L. Hollberg, W. M. Itano, S. R. Jefferts, M. J. Delaney, K. Kim, F. Levi, T. E. Parker, and J. C. Bergquist, Phys. Rev. Lett. **97**, 020801 (2006).
[3] J. J. Thorn, E. A. Schoene, T. Li, and D. A. Steck, Phys. Rev. Lett. **100**, 240407 (2008).
[4] P. D. Lett, W. D. Phillips, S. L. Rolston, C. E. Tanner, R. N. Watts, and C. I. Westbrook, J. Opt. Soc. Am. B **6**, 2084 (1989).
[5] J. Dalibard and C. Cohen-Tannoudji, J. Opt. Soc. Am. B **6**, 2023 (1989).
[6] R. Dum, P. Marte, T. Pellizzari, and P. Zoller, Phys. Rev. Lett. **73**, 2829 (1994).
[7] J. Cerrillo, A. Retzker, and M. B. Plenio, Phys. Rev. Lett. **104**, 043003 (2010).
[8] G. Poulsen, Y. Miroshnychenko, and M. Drewsen, Phys. Rev. A **86**, 051402 (2012).
[9] J. I. Cirac, P. Zoller, H. J. Kimble, and H. Mabuchi, Phys. Rev. Lett. **78**, 3221 (1997).
[10] H. J. Kimble, Nature (London) **453**, 1023 (2008).
[11] S. Nußmann, M. Hijlkema, B. Weber, F. Rohde, G. Rempe, and A. Kuhn, Phys. Rev. Lett. **95**, 173602 (2005).
[12] J. Bochmann, M. Mücke, C. Guhl, S. Ritter, G. Rempe, and D. L. Moehring, Phys. Rev. Lett. **104**, 203601 (2010).
[13] A. C. Dada, E. Andersson, M. L. Jones, V. M. Kendon, and M. S. Everitt, Phys. Rev. A **83**, 042339 (2011).
[14] C. F. Roos, D. Leibfried, A. Mundt, F. Schmidt-Kaler, J. Eschner, and R. Blatt, Phys. Rev. Lett. **85**, 5547 (2000).
[15] A. Reiserer, C. Nölleke, S. Ritter, and G. Rempe, arXiv:1212.5295 [physics.atom-ph].
[16] J. I. Cirac, M. Lewenstein, and P. Zoller, Phys. Rev. A **51**, 1650 (1995).
[17] S. Zippilli and G. Morigi, Phys. Rev. Lett. **95**, 143001 (2005).
[18] Z. Yi, W. J. Gu, and G. X. Li, Opt. Express **21**, 3445-3462 (2013).
[19] Y. Wu and X. X. Yang, Phys. Rev. A **71**, 053806 (2005).
[20] M. Bienert and G. Morigi, New. J. Phys. **14**, 023002 (2012).
[21] T. Kampschulte, W. Alt, S. Manz, M. Martinez-Dorantes, R. Reimann, S. Yoon, D. Meschede, M. Bienert, and G. Morigi, arXiv:1212.3814 [quant-ph].
[22] S. Zhang, C. W. Wu, and P. X. Chen, Phys. Rev. A **85**, 053420 (2012).
[23] J. I. Cirac, R. Blatt, P. Zoller, and W. D. Phillips, Phys. Rev. A **46**, 2668 (1992).
[24] S. Stenholm, Rev. Mod. Phys. **58**, 699 (1986).
[25] J. S. Peng and G. X. Li, *Introduction to Modern Quantum Optics* (World Scientific, Singapore, 1998).
[26] S. M. Tan, J. Opt. B: Quantum Semiclass. Opt. **4**, 424 (1999).
[27] A. B. Mundt, A. Kreuter, C. Becher, D. Leibfried, J. Eschner, F. Schmidt-Kaler, and R. Blatt, Phys. Rev. Lett. **89**, 103001 (2002).